International Journal of Hydrogen Energy 78 (2024) 984–990

Contents lists available at ScienceDirect

International Journal of Hydrogen Energy

journal homepage: www.elsevier.com/locate/he

Nitrogen oxides removal from hydrogen flue gas using corona discharge in marine boilers: Application perspective

Dominik Kreft [a,*], Konrad Marszałkowski [a], Karol Szczodrowski [b]

[a] Faculty of Mechanical Engineering and Ship Technology, Gdańsk University of Technology, Gdańsk, Poland
[b] Institute of Experimental Physics, University of Gdańsk, Gdańsk, Poland

ARTICLE INFO

Keywords:
Hydrogen flue gas
Nitrogen oxides
Corona discharge
Air pollution
NO_x removal

ABSTRACT

This paper focuses on the combustion of hydrogen in boilers, as it appears to be a more effective method than using fuel cells for heating purposes due to higher boiler efficiency. One of the main disadvantages of hydrogen combustion in air is NO_x formation. Therefore, the authors decided to introduce corona discharge as an innovative technique to clean hydrogen flue gas by effectively reducing NO_x levels. The method involves generating positive plasma at atmospheric pressure by applying up to a 23 kV voltage difference between rod and ring-shaped electrodes. Experimental studies have shown that corona discharge can significantly lower the concentrations of NO and NO_x in exhaust gases. The maximum $DeNO_x$ level was found to be 32.3%, while the plasma generator uses 17.5% of the power contained in burned hydrogen. The findings suggest that this technology holds potential for application in industrial hydrogen combustion systems, offering an environmentally friendly alternative to conventional NO_x reduction methods.

1. Introduction

With the growing concern for climate change and the need for sustainable energy sources, hydrogen has emerged as a promising alternative to traditional fossil fuels. However, the combustion of hydrogen can still result in the emission of nitrogen oxides, which contribute to air pollution and have detrimental effects on human health and the environment. This article aims to present corona discharge as a novel technique to clean hydrogen flue gas by effectively reducing NO_x levels.

Hydrogen as a fuel offers many positive features such as very high energy density, wide flammability range, no emission of CO_2 or SO_x, it is not a fossil fuel, can be manufactured in several ways and is one of the most sustainable fuels. Unfortunately, there are also some engineering challenges such as fire and explosion safety, high volume of storage in pressurized form, low temperature of storage in liquefied form, and losses through the walls of the receiver/boil-off gas.

The manufacturing of hydrogen has three main degrees of environmental impact. The synthetic cracking of hydrocarbon chains in fossil fuels produces gray hydrogen. If the CO_2 during the process is captured and stored it is called blue hydrogen. The most environmentally friendly is green hydrogen, made by electrolysis of water using a renewable source of energy. As green hydrogen is the most expensive, its share in global production is only 4% [1]. High hopes are made for the development of nuclear thermolysis hydrogen generators.

There are two main ways to use hydrogen as a fuel. The first is electrochemical by fuel cells directly producing direct current. The second is combustion for thermal energy demanded by boilers or engines. The paper focuses on the combustion of hydrogen in boilers as it seems to be a more effective way than using fuel cells in boilers. The thermal efficiency of marine fired boilers is 92–98% [2]. Using fuel cells for the same purpose, the boiler would be heated by electricity, which will be generated from hydrogen. Electrically heated boiler efficiency could be up to 100%, but the efficiency of popular PEM fuel cells is only up to 60% [3,4]. On the other hand, one of the main disadvantages of hydrogen combustion in the air is NO_x formation. If there will be a more effective method of NO_x removal, the combustion of hydrogen could be reasonable. It should be mentioned that there are also some engineering challenges with hydrogen-fueled boilers such as high combustion temperature, fast flame propagation (flashback possibilities), operation safety, and hydrogen supply. Most studies focus on pure hydrogen's impact on the atmosphere, caused by hydrogen leakage from the distribution system, and do not analyze the combustion of hydrogen as assuming its usage only by fuel cells [5–7]. This is why the authors decided to investigate the NO_x formation process and exhaust gas

* Corresponding author.
E-mail address: domkreft@pg.edu.pl (D. Kreft).

https://doi.org/10.1016/j.ijhydene.2024.06.385
Received 4 June 2024; Received in revised form 25 June 2024; Accepted 27 June 2024
Available online 2 July 2024

cleaning method from hydrogen combustion using corona discharge.

Considering the shipping industry there are global limits on NO_x emission in the emission control area (ECA) for combustion engines. Since 2016 these limits are in Tier III depending on n = rated engine speed (rpm) and are:

- 3.4 g/kWh when n is less than 130 rpm,
- $9 \cdot n^{-0.2}$ g/kWh when n is 130 or more but less than 2000 rpm,
- 2.0 g/kWh when n is 2000 rpm or more [8].

There is a lack of regulations for NO_x emission from fired boilers (especially from hydrogen-fueled boilers, which, apart from pilot studies, are not utilized on ships yet) as their emissions are only a small part of the ship's total emission. Such legislation may emerge in the future.

2. Nitrogen oxide formation

The hydrogen generator consists of two tanks containing electrodes. Tanks are filled with a 15% water solution of sodium hydroxide (NaOH). The following chemical reactions occur during the electrolysis of water solution of active metals hydroxides:

- Oxidation at the anode (+)

$$4OH^- \rightarrow O_2 + 2H_2O + 4e$$

- Reduction at the cathode (−)

$$4H_2O + 4e \rightarrow 2H_2 + 4OH^-$$

- Overall redox reaction

$$2H_2O \rightarrow O_2 + 2H_2$$

The gasoeus products from both electrodes are mixed, making the addition of air unnecessary, as the stoichiometry of the gas mixture is optimal for combustion. Such gas is commonly called HHO (Hybrid Hydrogen Oxygen). From the electrodes, gas flows to the small pressure tank and to the burner nozzle. The combustion of hydrogen is one of the simplest processes, and in the atmosphere of pure oxygen it leads to the reaction:

$$2H_2 + O_2 \rightarrow 2H_2O$$

In the case of the hydrogen combustion taking place in air, the additional processes involving the air components, mostly nitrogen, as reactants have to be taken into account.

The hydrogen burns at a temperature exceeding 2000 °C, while thermal NO_x formation occurs at temperatures above 750 °C, so emission of NO_x during hydrogen combustion occurs similarly as in the case of combustion of fossil fuels. The combustion temperature is closely tied to nitric oxide formation [9,10]. As shown at Fig. 1 the hotter flame the more nitrogen oxides are produced. Error bars represent one standard deviation of the mean (similarly for the next figures).

The combustion causes the splitting of normally stable molecules apart and the following reactions of nitrogen oxide formation appears [11]:

$$N_2 + O \overset{k_1}{\Rightarrow} NO + N$$

$$N + O_2 \overset{k_2}{\Rightarrow} NO + O$$

$$N + OH \overset{k_3}{\Rightarrow} NO + H$$

Where k is the rate constants of nitrogen oxide formation reactions in $m^3 \cdot kmol^{-1} \cdot s^{-1}$ and according to Ref. [12], they are respectively:

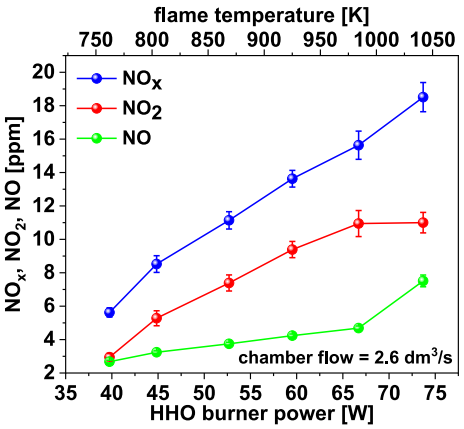

Fig. 1. NO, NO_2 and NO_x quantity as a function of burner power.

$$k_1 = 3.1 \bullet 10^{10} \bullet e^{\frac{-160}{T}}$$

$$k_2 = 6.4 \bullet 10^{6} \bullet Te^{\frac{-3125}{T}}$$

$$k_3 = 4.2 \bullet 10^{10}$$

Other rate constants resulting from experimental studies can be found in the [13] book.

Afterward, nitric oxide connects with oxygen, and nitrogen dioxide is formed.

$$2NO + O_2 = 2NO_2$$

Nitrogen dioxide is a yellow to brown asphyxiant gas depending on the temperature. It is also a strong oxidizing agent and a poison that irritates the respiratory tract. By reaction with water, nitric acids are formed due to the disproportionation of nitrogen dioxide [14]:

$$2NO_2 + H_2O = HNO_3 + HNO_2$$

Spontaneously nitrogen dioxide could convert into dinitrogen tetroxide at a temperature over 147 °C.

$$2NO_2 \leftrightarrows N_2O_4$$

The process of NO formation is an exponential function of temperature. The amount of NO produced over time can be determined using the extended Zeldovich mechanism calculation, provided that the oxygen concentration is assumed to be greater than the equilibrium level:

$$\frac{d[NO]}{dt} = 6 \bullet T^{-0.5} 10^{16} e^{\frac{-69090}{T}} \bullet [O_2]^2 [N_2]$$

Where T is temperature in K and $[NO/O_2/N_2]$ is the equilibrium concentration of respective chemical species in $mol \cdot cm^{-3}$ [15,16].

3. Nitrogen oxide removal

As the combustion temperature has a significant impact on NO_x formation, there are a few mechanisms to reduce it. In modern engines, the basic method is changing the fuel-air mixture to obtain lean-burn conditions and usage of Exhaust Gas Recirculation (EGR) where some part of cooled exhaust gas are flowing back to the combustion chamber. Most of burners have a special design to reduce the burning temperature [17,18]. However, reducing thermal NO_x emission can lead to a reduction of desired parameters such as energy output (mechanical energy in combustion engines or thermal energy in boilers), overall efficiency, and increased emission of other gases (ex. Hydrocarbons). Therefore the hydrogen boiler designer has to find a balance between NO_x emission and a reduced level of performance which generates increased operating costs.

There are an array of technologies for the after-treatment of exhaust gases to reduce NO_x emissions. In the maritime industry, the most common is selective catalytic reduction (SCR). For vehicles beyond SCR, these are three-way catalytic converters (TWC) and lean NO_x traps (LNT) which are most often combined for the best exhaust gas purification. All mentioned methods are capable to reduce NO_x levels from hydrogen exhaust gas as well as from fossil fuels exhaust gas. Unfortunately, they increase investment costs, operational costs, and system complexity.

The average investment cost of SCR reactors, which are most commonly used in the maritime industry, is $45 per kW of engine nominal power, while the operational cost is $940 per ton of NO_x [19]. It is difficult to compare the investment cost of a plasma reactor because there is a lack of full-scale reactors existing on board. However, it can be assumed that the cost will be lower because SCR requires an entire urea system. The main operational costs of SCR are for urea and electricity, which can be estimated at $0.005 per kWh, while the operational cost for the plasma reactor $0.02 per kWh [20].

The method proposed in this paper is the low-energy corona discharge set in the hydrogen exhaust gas manifold. Plasma is generated at the atmospheric pressure, by applying a high potential difference between two electrodes where one has a sharp tip. Due to the electric discharge, the exhaust gas is ionized around the thinnest electrode. The intensity of the discharge depends on the air gap, the potential difference, pulse frequency, the shape of the electrodes, and the medium property in which the discharge is located [21,22]. There can be distinguished the positive and negative corona discharge according to the voltage polarity. Positive corona discharges have lower free electron density. However, the electrons in a positive corona discharge contain more energy and are more concentrated, which is why negative corona discharges are optically bigger than positive ones [23].

One can assume that the combustion products of a hydrogen burner consist of N_2, O_2, H_2, H_2O, NO and NO_2. CO and CO_2 may be omitted due to their low concentrations in the air. Chemical reactions during the gas flow through the corona reactor can be divided into 3 stages [24]:

1. Discharge Stage: High-energy electrons bombard gas molecules, breaking covalent bonds, creating free radicals, and exciting decomposed atoms to an unstable state.
2. Post-discharge Stage: Excited-state atoms from the first stage collide with gas molecules, generating secondary radicals. These radicals then interact with other particles, leading to quenching or the generation of new radicals.
3. Free Radicals React with NO_x Stage: reaction of the free radicals with NO_x.

The operating principle of corona discharge treatment is similar to electron beam treatment because both techniques result in a significantly larger portion of electrical energy going into the production of electrons, rather than into gas heating [25].

The Fig. 2 illustrates the reaction mechanism in the corona discharge chamber. Subsequently, the formed free radicals react with other species, creating new compounds. In the reactor chamber, there are several dozen different chemical reactions. The most important ones are as folows [24]:

$$e + NO \rightarrow e + \cdot O + \cdot N \quad \text{(R1)}$$

$$e + NO_2 \rightarrow e + NO + \cdot O \quad \text{(R2)}$$

$$e + H_2O \rightarrow e + \cdot OH + \cdot H \quad \text{(R3)}$$

$$\cdot O + NO \rightarrow NO_2 \quad \text{(R4)}$$

$$\cdot N + NO \rightarrow N_2 + \cdot O \quad \text{(R5)}$$

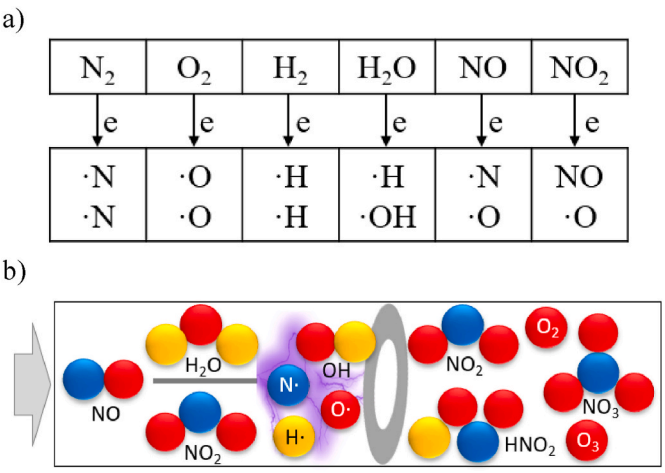

Fig. 2. a) Reacion mechanism in corona chamber b) Graphic diagram of the main NO_x reduction reactions, where O atoms are red, N atoms are blue, and H atoms are yellow. (For interpretation of the references to colour in this figure legend, the reader is referred to the Web version of this article.)

$$\cdot OH + NO \rightarrow HNO_2 \quad \text{(R6)}$$

$$\cdot O + NO_2 \rightarrow NO + O_2 \quad \text{(R7)}$$

$$\cdot N + NO_2 \rightarrow N_2 + O_2 \quad \text{(R8)}$$

$$\cdot OH + NO_2 \rightarrow HNO_3 \quad \text{(R9)}$$

$$\cdot O + O_2 \rightarrow O_3 \quad \text{(R10)}$$

$$NO + O_3 \rightarrow NO_2 + O_2 \quad \text{(R11)}$$

$$NO_2 + O_3 \rightarrow NO_3 + O_2 \quad \text{(R12)}$$

The equations R1 – R3 represent the reactions occurring in the Discharge Stage and describe the dissociacion of the molecules of nitrogen oxides (R1, R2) and water (R3) by the high-energy electrons. The radicals created during this process are involved in subsequent reactions with other chemical species present in the system and occur in the Post-discharge Satage. However, in the case of the part of these reactions where the radicals react with nitrogen oxides (R4 – R9) the Free Radicals React with NO_x Stage can be distinguished as a stage that determines the concentration of NO_x. Taking into account the aim of the work the reactions R5, R6, R8 and R9 are involved in the diminishing of the nitrogen oxides concentration.

The focus of the present solution is the plasma generation across the entire cross-section of the reactor, hence a single electrode in the form of an adjustable-length rod was employed. The selection of a single electrode is justified by the ease of achieving maximum intensity of corona discharge in the stream of hydrogen exhaust without arc ignition. Previous studies [26] demonstrate the highest efficiency in NO_x removal in Dielectric Barrier Discharge Plasma Reactors with multipoint electrodes. Similarly effect, applies to the polarity of the ionizing electrode. Under positive biasing, the generated plasma is more intense, less susceptible to arcing and breakdown. That is why in the experiment, the corona discharge was positive (+ on the rod electrode), as in comparison, the negative corona was found to have a smaller effect on the denitrification ($DeNO_x$) in the same conditions [27,28]. It is well known that after corona treatment the concentration of NO decreases, but the concentration of NO_2 increases, as NO is oxidized to NO_2. The effect intensifies when the applied discharge voltage rises [29]. The overall NO_x balance is negative, due to the fact that a portion of the NO_x is transformed through its interaction with OH radicals in the plasma reactor [30].

The humidity of flue gases significantly affects the interaction of

corona discharge in the $DeNO_x$ process. Water molecules absorb electrons in the coronas and turn into slow negative ions. They affect the discharge characteristics – lower the discharge current and reduce corona region. Under higher humidity conditions at the same discharge power, the efficiency of $DeNO_x$ is increased. This is because oxygen with higher relative humidity supplies more H_2O molecules, leading to the production of additional OH radicals. Consequently, more NO_x molecules are converted into HNO_x molecules at the same power level [29]. Many research confirms that the efficiency of $DeNO_x$ can be increased by adding a catalyst made of Ag_2O or TiO_2 into the reactor or by injecting an NH_3 solution (SCR) [31–33].

4. Apparatus and methods

Several experimental studies have been conducted to investigate the NO_x removal efficiency of corona discharge in hydrogen flue gas. These studies involve the design and construction of reactor, where various parameters such as voltage, flame temperature, gas flow rate, and electrode configuration are optimized. The experiments typically measure the NO_x removal efficiency and evaluate the influence of different operating conditions on the process. The proposed NO_x removal method was tested at a laboratory station shown in Fig. 3. The process reactor is a tube made of transparent polycarbonate with a diameter of 100 mm and a lencgth of 2 m. The section conneacting the HHO burner to the polycarbonate tube is made of stainless steel tubing and tightly connects at the bottom of the reactor. The hydrogen-oxygen mixture is prepared in an electrolyzer and stored under pressure in a tank. The pressure of the HHO supplied to the burner is stabilized using a precise and leak-free pressure regulator. The power of the NO_x emitter burner (and consequently the flame temperature) is controlled using a proprietary precise mechanism that regulates the burner valve. A microcontroller-based system ensures repeatability of the valve opening degree.

To generate corona discharge between electrodes, a flyback pulse converter with a frequency of 50 ± 3 kHz was employed. The flame temperature was measured using a type K thermocouple positioned 25 mm above the burner nozzle. The three measurement points of the flue gas analyzer were located at 240, 655, and 1040 mm above the plasma reactor, respectively. At the top of the reactor, a regulated fan was installed, which prevented water vapor from condensing on the reactor walls and ensured a constant flue gas flow of 2.6 or 3.1 $dm^3\ s^{-1}$. Water caused disturbances in measurement and made it impossible to achieve a steady state reactor operation.

The active experiment was conducted according to a static predetermined research plan, in which for each measurement point covering specific HHO pressure, a series of five repetitions were carried out. Each repetition comprised one full cycle of filling and emptying the tank with the HHO mixture. The pressure in the HHO generator tank is maintained using a pressure switch with a hysteresis of 50 kPa. Similarly, measurements were made for changes in plasma intensity. The obtained results of nitrogen oxides concentration, measured using an electrochemical exhaust gas analyzer Testo 350, represent the arithmetic mean for each measurement point consisting of five repetitions, with the exhaust gas analyzer (EGA) sampling every 10 s.

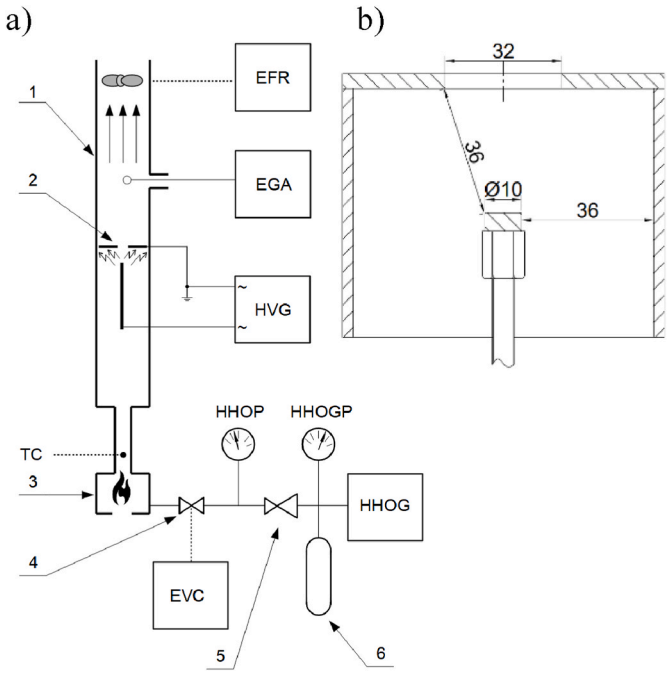

Fig. 3. a) NOx removal laboratory station diagram. 1 - process reactor column, 2 - ring HV electrode, 3 - exhaust gas emitter, 4 - proportional valve controller, 5 - leak-free pressure regulator, 6 - pressure tank for HHO, EFR - electronic fan speed controller, EGA - exhaust gas analyzer, EVC - electronic valve controller, HHOG - electrolytic hydrogen-oxygen mixture generator, HHOP - pressure supplying the burner, HHOG - pressure in the HHO generator tank, HVG - high voltage generator, TC - thermocouple, b) high voltage electrode detail.

5. Result and discussion

The results of the study on the influence of the pressure and temperature of burnt HHO on the amount of nitrogen oxides produced are shown in Fig. 4 a) for NO_x, b) for NO_2, and c) for NO. All cases were studied with the plasma reactor turned on and off for two different exhaust flow rates in the chamber. For all nitrogen oxides, it is noticeable that at an exhaust flow rate of 2.6 $dm^3\ s^{-1}$, higher concentrations are observed compared to 3.1 $dm^3\ s^{-1}$, as the exhaust gases are less diluted with air by fan. Each nitrogen oxide content increases with the increase in HHO burner pressure and thus the flame temperature. Comparing the amount of nitrogen oxides with the plasma reactor operating at 21 kV (12.9 W) to the reference conditions, it can be found that the NO amount has practically dropped to zero for all HHO pressures. Additionally, with the plasma generator turned on, a significant increase in NO_2 is observed on chart b). Despite this, on chart a), it can be seen that the concentration of NO_x, which is the sum of NO and NO_2, decreases when the plasma reactor is turned on for concentrations higher than 10 ppm for an exhaust flow rate of 2.6 $dm^3\ s^{-1}$ and for concentrations higher than 8 ppm for an exhaust flow rate of 3.1 $dm^3\ s^{-1}$. For the lower fan rotation speed and burner set at 100 kPa, the NO_x concentration was measured at 18.95 ppm, while after starting the plasma reactor, this value dropped to 15.98 ppm. An important fact is that for low NO_x contents in the tested gas, the activation of the plasma generator results in an increase of their concentration. On graph a), these points are marked as purification starting points. The Fig. 4 d) shows the change in temperature and NO_x content in exhaust gases depending on the distance of the measurement location from the plasma reactor. It can be observed that, as expected, the temperature of the exhaust gases decreases as the distance from the reactor increases. With the plasma reactor operating at 21 kV, the temperature was correspondingly higher than when it was turned off, due to the additional heating of the gases by the corona discharge. The decrease of NO_x concentration is also evident due to the higher dilution of exhaust gases in the upper part of the chamber. With the corona discharge activated, it can be observed that both blue curves are not parallel, and for closer distances to the reactor, the cleaning rate was higher than for farther distances. This is due to two factors. Firstly, for lower concentrations, NO_x plasma removal has a smaller effect or may even have a reverse effect, generating additional NO_x. Secondly, during the ionization of exhaust gases, free radicals had the most time to react when the NO_x content was measured at a distance of 1040 mm from the reactor.

Using a hygro-thermo-meter, the humidity and gas temperature were measured under the same conditions: HHO pressure 100 kPa, exhaust gas flow rate 2.6 $dm^3\ s^{-1}$, and corona discharge voltage 21 kV. The

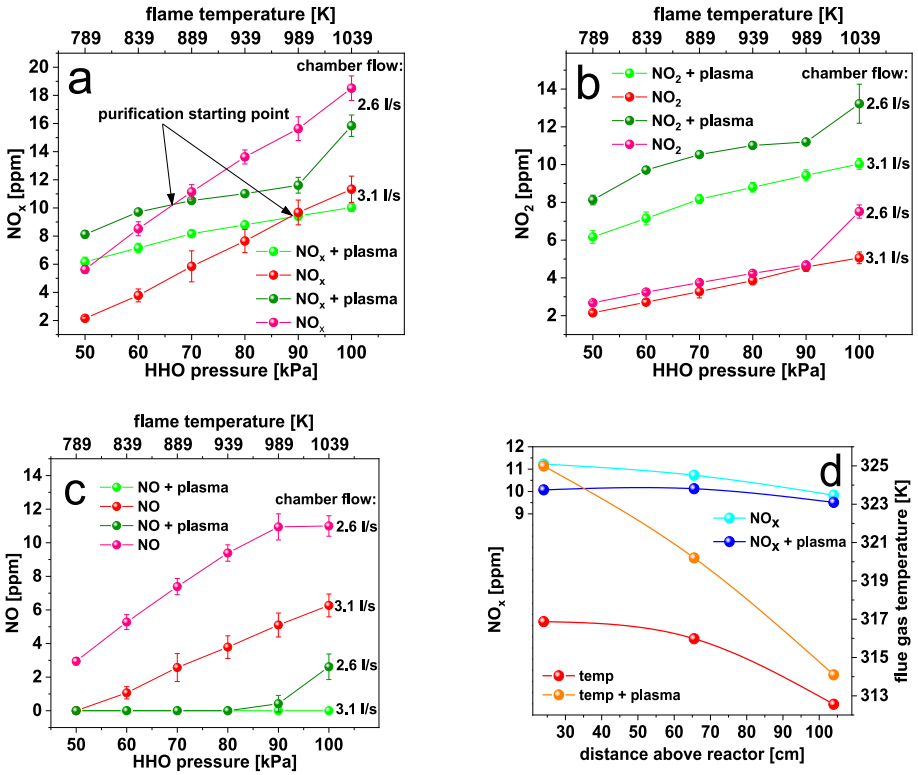

Fig. 4. Nitrogen oxides reference ammount and with activated plasma reactor, a) NO_x, b) NO_2, c) NO. d) NO_x amount and exhaust gas temperature depending on the measurement distance from the reactor.

results are presented in Table 1.

It can be seen that after starting the plasma generator, the gas temperature increased, as shown in Fig. 4 d). The absolute humidity decreased because part of the water vapor was broken down into oxygen and hydroxy radicals (R3), forming new chemical compounds. Additionally, based on the Mollier chart (assuming that the exhaust gases of the HHO burner are treated as moist air), the gas enthalpy can be approximately determined, which increased by 2.58 kJ/kg after turning on the plasma generator.

The power consumed by the plasma generator and the HHO generator was measured using electrical meters, and the efficiency of both devices was taken into account in all calculations. The efficiency of the HHO burner was determined using a calorimeter and is equal to $\eta_b = 23.5 \pm 4$ %, while efficiency of plasma generator was calculated based on voltage drop on each generator component: $\eta_{pg} = 60 \pm 5$ %. The dependence of the plasma generator's power on the corona discharge voltage is shown in Fig. 5 a). When the voltage was below 15 kV, corona discharge was not visible, while above 22 kV, with an air gap of 36 mm, an electric arc ignited, so this value was assumed to be the maximum possible for testing. The long-term safety operation has been estimated at 21 kV. Oscilloscope testing showed that the current frequency for the high-voltage part of the plasma generator was 50 ± 3 kHz, which was constant for all voltage values. The Fig. 5 b) shows the relative change in NO_x content after activating the plasma generator at 21 kV voltage for two exhaust flow rates as a function of the Specific Energy Density (SED) of the HHO generator. The flow rate of 2.6 $dm^3\ s^{-1}$ was characterized by a higher NO_x content. At SED value of 19.5 J dm^{-3}, a cleaning effect was achieved with the maximum value of 25.7% for HHO SED equal to 25.5 J dm^{-3}. On the other hand, for a higher exhaust gas flow rate at a low SED value, the NO_x removal efficiency become negative by over 175% as it was confirmed in paper [24]. The cleaning effect was only achieved for SED HHO = 25.5 J dm^{-3}. The Fig. 5 c) shows the relative change in NO_x content as a function of the plasma generator's SED for an exhaust gas flow rate of 2.6 $dm^3\ s^{-1}$, HHO pressure of 100 kPa, and flame temperature of 1039 K. s the corona discharge voltage (and thus SED) increases, the relative NO_x removal value increases, indicating a positive correlation between the plasma generator's operating parameters and the efficiency of NO_x removal. The dashed line marks the SED value above which (blue points) the NO content became lower than the NO_2 value in the examined exhaust gases. The measurement points are described using a second-order approximating function with a 95% confidence band marked. The maxiumum removal efficiency for 4.95 SED (22 kV plasma voltage) was 32.3 %.

Table 1
The temperature, absolute humidiy and enthalpy of hydrogen exhaust gases.

	T [K]	x [g·m^{-3}]	i [kJ·kg^{-1}]
Athmosphere	299.25	7	44.12
Without plasma	312.65	13.5	74.51
With plasma	317.65	12.5	77.09

6. Summary and conclusion

Experimental investigation was conducted to remove NO_x from hydrogen exhaust gas with corona discharge system and the following conclusions have been obtained:

- The exhaust gases of hydrogen subjected to plasma treatment change their composition. NO decreases, NO_2 increases, but their total NO_x also decreases.
- The maximum investigated level of $DeNO_x$ was 32.3% for a plasma SED of 4.95, during the SED of the HHO generator was over 28 J dm^{-3}.
- The distance of NO_x concentration measurement from the reactor is significant due to the dilution of exhaust gases and the prolonged interaction of free radicals in hydrogen flue gas.

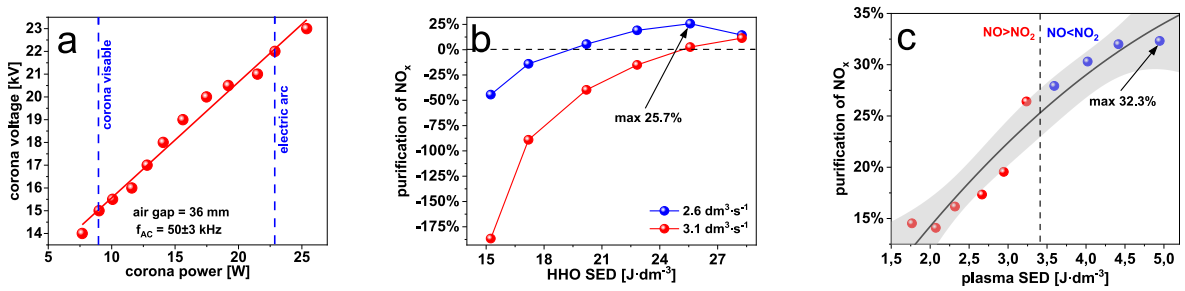

Fig. 5. a) Plasma voltage in the function of energy flow, NO_x relative purification rate depending on b) the hydrogen burner specific energy density, c) plasma generator specific energy density with a second-order approximating function and 95% convidence band.

- The initial concentration of NO_x in the exhaust gases is very significant. At low NO_x concentrations (below 8–10 ppm) in the exhaust gases, activating the plasma generator results in negative removal efficiency.

Corona discharge presents a promising approach for cleaning hydrogen flue gas from nitrogen oxides. The technology's ability to remove NO_x efficiently, coupled with its compatibility with existing systems, makes it an attractive option for mitigating the environmental impact of hydrogen boilers. Future research efforts should focus on addressing the challenges associated with corona discharge, such as reactor design optimization and cost-effective scaling, to enable its widespread adoption in industrial settings. It should also investigate $DeNO_x$ for higher concentrations and compare the obtained results with the impact of UV light on NO_x reduction using different wavelengths.

Funding

This work was supported by the Gdańsk University of Technology [grant IDUB Argentum 2022].

CRediT authorship contribution statement

Dominik Kreft: Writing – review & editing, Writing – original draft, Supervision, Project administration, Investigation, Conceptualization. **Konrad Marszałkowski:** Writing – review & editing, Investigation, Data curation, Conceptualization. **Karol Szczodrowski:** Writing – review & editing, Validation, Methodology.

Declaration of competing interest

The authors declare that they have no known competing financial interests or personal relationships that could have appeared to influence the work reported in this paper.

References

[1] Molloy P, Baronett L. "Hard-to-abate" sectors need Hydrogen. 2019.
[2] Giernalczyk M, Górski Z. Siłownie okrętowe cz.2 Instalacje okrętowe. Gdynia: Akademia Morska w Gdyni; 2011.
[3] Özgür T, Yakaryılmaz AC. A review: exergy analysis of PEM and PEM fuel cell based CHP systems. Int J Hydrogen Energy 2018;43:17993–8000. https://doi.org/10.1016/j.ijhydene.2018.01.106.
[4] Taner T. The novel and innovative design with using H2 fuel of PEM fuel cell: efficiency of thermodynamic analyze. Fuel 2021;302. https://doi.org/10.1016/j.fuel.2021.121109.
[5] Derwent R, Simmonds P, O'Doherty S, Manning A, Collins W, Stevenson D. Global environmental impacts of the hydrogen economy. Int J Nucl Hydrogen Prod Appl 2006;1:57. https://doi.org/10.1504/ijnhpa.2006.009869.
[6] Lakshmanan S, Bhati M. Unravelling the atmospheric and climate implications of hydrogen leakage. Int J Hydrogen Energy 2024;53:807–15. https://doi.org/10.1016/j.ijhydene.2023.12.010.
[7] Popa ME, Segers AJ, Denier van der Gon HAC, Krol MC, Visschedijk AJH, Schaap M, et al. Impact of a future H2 transportation on atmospheric pollution in Europe. Atmos Environ 2015;113:208–22. https://doi.org/10.1016/j.atmosenv.2015.03.022.
[8] International Maritime Organization. Resolut. Mepc 2014;251(66):1–12. 251.
[9] Zel'dovich YB. The oxidation of nitrogen in combustion explosions. Acta Physicochimica USSR 1946;21:577–628.
[10] Abdelhafez A, Abdelhalim A, Abdulrahman GAQ, Haque MA, Habib MA, Nemitallah MA. Stability, near flashback combustion dynamics, and NOx emissions of H2/N2/air flames in a micromixer-based model gas turbine combustor. Int J Hydrogen Energy 2024;61:102–12. https://doi.org/10.1016/j.ijhydene.2024.02.297.
[11] Lewis AC. Optimising air quality co-benefits in a hydrogen economy: a case for hydrogen-specific standards for NO x emissions. Envir Sci: Atmosphere 2021;1:201–7. https://doi.org/10.1039/d1ea00037c.
[12] Homann K, Wagner H. Some aspect of soot formation. Gordon and Breach Publishers; 1996.
[13] Merkisz J, Piasecznу L, Kniaziewicz T. Zagadnienia emisji spalin silników okrętowych. Poznań: Wydawnictwo Politechniki Poznańskiej; 2016.
[14] Stapf H. Podstawy chemii i technologii dla zatrudnionych w przemyśle. Warszawa: PWT; 1953.
[15] Merkisz J. Wpływ motoryzacji na skażenie środowiska naturalnego. Poznań: wydawnictwo politechniki poznańskiej. 1993.
[16] Sher E. Handbook of air pollution from internal combustion engines. first ed. Beersheba: Elsevier; 1998.
[17] Lamas MI, Rodríguez CG. Emissions from marine engines and NOx reduction methods. J Marit Res 2012;9:77–82.
[18] Barreiro P, Alava I, Blanco JM, Lopez-Ruiz G. An assessment of the operating conditions of the micromix combustion principle for low NOx industrial hydrogen burners: numerical and experimental approach. Int J Hydrogen Energy 2024;66:208–22. https://doi.org/10.1016/j.ijhydene.2024.04.052.
[19] Zhang G, Yan H, Li T, Zhu Y, Zhou S, Feng Y, et al. Relation analysis on emission control and economic cost of SCR system for marine diesels. Sci Total Environ 2021;788. https://doi.org/10.1016/j.scitotenv.2021.147856.
[20] Penetrante BM. Economics of electron beam and electrical discharge processing for post-combustion NOx control in internal combustion engines. CA (United States): Lawrence Livermore National Lab.; 1993.
[21] Moreau E, Audier P, Benard N. Ionic wind produced by positive and negative corona discharges in air. J Electrost 2018;93:85–96. https://doi.org/10.1016/j.elstat.2018.03.009.
[22] Chang JS, Lawless PA, Yamamoto T. Corona discharge processes. IEEE Trans Plasma Sci 1991;19:1152–66. https://doi.org/10.1109/27.125038.
[23] Wu Y, Lei L, Zhang J, Ge D, Zhang J. Analysis of current characteristics of corona discharge in high voltage transmission. IOP Conf Ser Earth Environ Sci 2020;440. https://doi.org/10.1088/1755-1315/440/3/032040.
[24] Wang Z, Kuang H, Zhang J, Chu L, Ji Y. Nitrogen oxide removal by non-thermal plasma for marine diesel engines. RSC Adv 2019;9:5402–16. https://doi.org/10.1039/c8ra09217f.
[25] Penetrante BM, Hsiao MC, Bardsley JN, Merritt BT, Vogtlin GE, Wallman PH, et al. Electron beam and pulsed corona processing of volatile organic compounds in gas streams. Pure Appl Chem 1996;68:1083–7. https://doi.org/10.1351/pac199668051083.
[26] Takaki K, Shimizu M, Mukaigawa S, Fujiwara T. Effect of electrode shape in dielectric barrier discharge plasma reactor for NOx removal. IEEE Trans Plasma Sci 2004;32:32–8. https://doi.org/10.1109/TPS.2004.823973.
[27] Fujii T, Kaneda Y, Rea M. NOx treatment test by positive DC corona reactor with and without water. Tran Inst Od Fluid Flow Mach 2000;107:45–53.
[28] Molchanov O, Krpec K, Horák J, Kubonová L, Hopan F, Ryšavý J. Combined control of PM and NOx emissions by corona discharge. Sep Purif Technol 2024;345. https://doi.org/10.1016/j.seppur.2024.127359.
[29] Lin H, Gao X, Luo Z, Cen K, Huang Z. Removal of NOx with radical injection caused by corona discharge. Fuel 2004;83:1349–55. https://doi.org/10.1016/j.fuel.2004.01.004.
[30] Krishna R, Bulusu M, Wandell RJ, Gallan RO, Locke BR. Nitric oxide scavenging of hydroxyl radicals in a nanosecond pulsed plasma discharge gas–liquid reactor. J Phys D Appl Phys 2019;52:504002.

[31] Miessner H, Francke K-P, Rudolph R, Hammer T. NOx removal in excess oxygen by plasma-enhanced selective catalytic reduction. Catal Today 2002;75:325–30. https://doi.org/10.1016/S0920-5861(02)00085-8.
[32] Paulauskas R, Jogi I, Striugas N, Martuzevičius D, Erme K, Raud J, et al. Application of non-thermal plasma for NOx reduction in the flue gases. Energies 2019;12. https://doi.org/10.3390/en12203955.
[33] Jiang B, Zhao S, Wang Y, Wenren Y, Zhu Z, Harding J, et al. Plasma-enhanced low temperature NH3-SCR of NOx over a Cu-Mn/SAPO-34 catalyst under oxygen-rich conditions. Appl Catal, B 2021;286. https://doi.org/10.1016/j.apcatb.2021.119886.